Journal of Alloys and Compounds 509 (2011) 4682–4687

Contents lists available at ScienceDirect

Journal of Alloys and Compounds

journal homepage: www.elsevier.com/locate/jallcom

Synthesis and microwave absorbing properties of polyaniline/$MnFe_2O_4$ nanocomposite

Seyed Hossein Hosseini [a,*], S.H. Mohseni [b], A. Asadnia [c], H. Kerdari [d]

[a] Department of Chemistry, Islamic Azad University, Islamshahr branch, Tehran,Iran
[b] Communication Department, University of Science and Technology, Tehran,Iran
[c] Department of Chemistry, Imam Hossein University, Tehran,Iran
[d] Department of Chemistry, Islamic Azad university, Saveh branch, Saveh, Iran

ARTICLE INFO

Article history:
Received 14 August 2010
Received in revised form
26 November 2010
Accepted 30 November 2010
Available online 7 December 2010

Keywords:
Microwave absorbing
Polyaniline
Nanocomposite
Mn ferrite

ABSTRACT

Conductive polyaniline (PANi)–manganese ferrite ($MnFe_2O_4$) nanocomposites with core–shell structure were synthesized by in situ polymerization in the presence of dodecyl benzene sulfonic acid (DBSA) as the surfactant and dopant and ammonium persulfate (APS) as the oxidant. The structure and magnetic properties of manganese ferrite nanoparticles were measured by using powder X-ray diffraction (XRD) and vibrating sample magnetometer (VSM), respectively. Its morphology, microstructure and DC conductivity of the nanocomposite were characterized by scanning electron microscopy (SEM), fourier transform infrared spectroscopy (FTIR) and four-wire-technique, respectively. The microwave absorbing properties of the nanocomposite powders dispersing in resin acrylic coating with the coating thickness of 1.4 mm were investigated by using vector network analyzers in the frequency range of 8–12 GHz. A minimum reflection loss of −15.3 dB was observed at 10.4 GHz.

1. Introduction

Microwave absorbing material plays a great role in electromagnetic pollution controlling, electromagnetic interference (EMI) shielding and stealth technology, etc. An "ideal" microwave absorbing material owns such advantages as tiny thickness, low density, wide band width and flexibility simultaneously. Spinal ferrites and hexagonal ferrites are well known as traditional granular microwave absorbers, but ferrite absorbent coatings have higher density and poor environmental stability, which restrict their wide applications as microwave absorbers. Conductive polymers are a new class of conductor, electromagnetic shielding and microwave absorbing materials, which show a number of advantages over traditional granular materials. Their composites with fillers, such as metal fibers, carbon black or carbon nano-fibers have been used as EMI shielding of electronic circuit and microwave absorbing materials [1–3]. Conductive polymer plays an important role in technologies such as stealth, electro static charge dissipation and EMI shielding [4]. Singh et al., synthesis of polyaromatic amine–ferromagnetic composite with nanosize TiO_2 (70–90 nm) and γ-Fe_2O_3 (10–15 nm) particles via in situ emulsion polymerization were reported. They were resulted polyaniline–TiO_2–γ-Fe_2O_3 nanocomposite has shown better shielding effectiveness due to absorption than the polyaniline–γ-Fe_2O_3 [5].

Among the known conducting polymers, polyaniline (PANi) has been intensively investigated as EMI shielding material and broad band microwave adsorbing material, due to some significant characteristics such as very light weight, flexibility and reasonably facile processibility [6]. The microwave properties of PANi are considerably influenced by their structural parameters, which are dependent on synthesis route doping method and dopant nature [7].

Enhanced microwave absorption properties in polyaniline and nanoferrite composite in X-band were studied by Gairola et al. too [8]. This work, highly conducting polyaniline nanocomposite with $Mn_{0.2}Ni_{0.4}Zn_{0.4}Fe_2O_4$ ferrite was prepared by mechanical blending. The complex permittivity, permeability and shielding effectiveness of the composite for different thicknesses were measured in the 8–12 GHz (X-band) frequency range. Microwave-absorbing properties of PANi/Ba ferrite were investigated by measuring complex permittivity, complex permeability and reflection loss in the 2–18 and 18–40 GHz microwave frequency range using the free space method. The results showed that a wider absorption frequency range could be obtained by adding different polyaniline contents in Ba ferrite [9]. One-step synthesis of α-FeOOH/polypyrrole (PPy) nanocomposites was reported by Xiao et al. [10]. The reflection loss evaluation based on the absorbing wall theory at the thickness of 2 mm showed that the nanocomposite at $[Py]/[Fe^{2+}] = 1.0$ exhibits the best microwave absorbing property in the 2–18 GHz. And the

* Corresponding author.
E-mail addresses: shhosseini@iiau.ac.ir, dr.shhosseini@gmail.com (S.H. Hosseini).

0925-8388/$ – see front matter © 2010 Elsevier B.V. All rights reserved.
doi:10.1016/j.jallcom.2010.11.198

corresponding reflection frequency range under −10 dB and −5 dB was 4.2 GHz and 5.8 GHz, respectively.

In the past decades, the spinel ferrites have been utilized as the most frequent absorbing materials in various forms. Manganese ferrite ($MnFe_2O_4$) is a common spinel ferrite material and has been widely used in microwave and magnetic recording applications [11]. Ferromagnetic fillers, such as different kinds of ferrites and carbonyl iron are generally used in composite absorbers [12]. Microwave absorbing structures typically consist of shaped materials with properties that allow electromagnetic (EM) waves to penetrate into regions where the electric and magnetic fields experience loss [13]. To compensate these defects, the integration of magnetic materials and conductive polymers has been investigated.

Zhao et al., microwave absorbing property and complex permittivity of the nano SiC particles doped with nitrogen within the frequency range of 8.2–18 GHz were investigated. They showed the reflection loss calculations show that the prepared nano SiC particles doped with nitrogen are good electromagnetic wave absorbers in the microwave range [14].

The carbonyl iron/$La_{0.6}Sr_{0.4}MnO_3$ composites were prepared by Cheng et al. and they also developed super-thin microwave absorbing materials [15]. They were indicated that carbonyl iron/$La_{0.6}Sr_{0.4}MnO_3$ composites may have an important application in wide band and super-thin electromagnetic absorbers in the frequency range of 8–12 GHz.

2. Experimental

2.1. Materials and instrumentals

Chemicals including metal salts, hexamethylene tetraamine (HMTA), potassium persulfate (KPS) and ethylene glycol (EG) are analytical grade (Merck) and were used without further purification. Water was deionized, doubly distilled, and deoxygenated prior to use. Styrene and methacrylic acid (analytical grade, Merck) were distilled to remove the inhibitor. Aniline monomer (analytical grade, Merck) was distilled twice under reduced pressure. DBSA and acrylic resin were of industrial grade. The other reagent, including ammonium persulfate (APS), was of analytical grade (Merck).

The morphology of coated particles and nanocomposite was observed scanning electron microscopy (SEM) with a JSM-6301F (Japan) instrument operated at an accelerating voltage of 10 kV. X-ray powder diffraction (XRD) patterns of the nanoparticles assembles were collected on a Philips-PW 1800 with Cu K radiation under Cu Kα radiation (λ = 1.5406 Å). Fourier transform infrared spectroscopy (FTIR) spectra were recorded on a PerkinElmer spectrum FTIR using KBr pellets. The M–H hysteresis loops were measured by vibrating sample magnetometer (VSM) (RIKEN DENSHI Co. Ltd., Japan). Microwave absorbing properties were measured by a Vector Network Analyzers (Agilent Technologies Inc. 8722) in the 8–12 GHz range at room temperature.

2.2. Preparation of nanoparticles

2.2.1. PS colloid

Negatively charged PS spheres with average diameter 230 nm, which were used as core particles, and were prepared by a free-emulsion polymerization method [16]. In a typical experiment, 10 mL styrene, 2 mL methacrylic acid and 0.054 g KPS were added to the flask with 100 mL deionized water. To eliminate oxygen effects the solution was purged with nitrogen before the process was initiated. The mixture was heated to 72 °C and stirred with a magnetic stirrer. The polymerization was continued for 24 h and in the whole procedure the nitrogen was purged. Concentration of PS spheres in solution is 80 mg/mL, which was calculated by drying 5 mL colloid solution and weighing the remained solids.

2.2.2. Coated particles

The coating procedure consisted of controlled hydrolysis of aqueous solutions of ferrous chloride and other divalent metal salts in the presence of polystyrene latexes. In a typical preparation process, 2 mL PS colloid solution was diluted with 250 mL deoxygenated distilled water and then mixed with the metal salts solution, which contained 10 mmol $FeCl_2$ and 5 mmol $MnCl_2$. After dispersed under ultrasonic for several minutes, the mixture was in corporate with 4 g HMTA and 0.5 g potassium nitrate and heated to 85 °C under gentle stirring. After 3 h, the system was cooled to room temperature. The solution was poured in to excess distilled waterand then magnetic particles were deposited using magnetic field. The precipitate was washed with distilled water for several times and then dried in oven at 80 °C for 24 h. In addition, to modify the surface chemical properties of the composites magnetic spheres, 5 mL ethylene glycol was added in to the reaction solution before the incorporation of HMTA.

2.3. Synthesis of $MnFe_2O_4$–PANi nanocomposite with core–shell structure

$MnFe_2O_4$–PANi core–shell nanocomposites were prepared by in situ polymerization in the presence of DBSA as the surfactant and dopant and APS as the oxidant. The DBSA was dissolved in distilled water with vigorous stirring for about 20 minand then $MnFe_2O_4$ nanoparticles (1.22 g) were added to the DBSA solution under stirring for approximately 1 h. Then 8 mL of aniline monomer was added to the suspension and stirred for 30 min. $MnFe_2O_4$ nanoparticles were dispersed well in the mixture of aniline/DBSA under ultra sonicaction for 2 h. 20 g APS in 60 mL-deionized water was slowly added dropwise to the mixture with a constant stirring. The polymerization with stirring under an ice-water bath was allowed to proceed for 4 h. The nanocomposite was obtained by filtering and washing the suspension with deionized water and ethanol, respectively. The obtained green-black powder with the content of 15 wt% $MnFe_2O_4$ was dried under vacuum for 24 h.

3. Results and discussion

3.1. X-ray diffraction

Fig. 1 shows the XRD pattern of manganese ferrites. It can be clearly noted from Fig. 1 that the ferrite shell are phase-pure cubic structure in all case according to the standard XRD patterns of the cubic ferrite Fe_3O_4 and $MnFe_2O_4$ standards, which is in good agreement with the JCPDS, No. 88-1965. The average crystallite size was calculated using software Originpro75 through the diffraction speaks from Scherer's formula as shown below:

$$D = \frac{0.89\lambda}{\beta \cos\theta}$$

where D is the crystal size, λ is the X-ray wave length, β is the broadening of the diffraction peak and θ is the diffraction angle. Calculated by the Scherrer formulation, the mean crystallite size of the ferrite particles is 24.27 nm.

As the data of the sample showed, the count rate will reflect the flux of diffracted X-ray photons for that orientation. Strong peaks are expected when the Bragg condition is satisfied:

$$n\lambda = 2d \sin\theta \quad (1)$$

where n is the order of diffraction (usually $n = 1$), λ is the X-ray wavelength and d is the spacing between planes of given Miller indices h, k and l. See references for more details concerning the Miller indices and the Bragg condition. In the cubic system, the plane spacing is related to the lattice constant a and the Miller indices by the following relation:

$$d = \frac{a}{\sqrt{h^2 + k^2 + I^2}} \quad (2)$$

Combining Eqs. (1) and (2), we get:

$$a = \frac{\lambda\sqrt{h^2 + k^2 + I^2}}{2 \sin\theta} \quad (3)$$

Thus for all sets of Miller indices there is an angle that will satisfy the Bragg condition such that the value of $\lambda/2a$ is a constant. The value of the lattice constant follows directly from the X-ray wavelength, which is 8.385 Å for this experiment. The strong and sharp peeks suggest that the as-synthesized products are well crystallized.

3.2. Magnetic properties

Fig. 2 (a) and (b) shows the magnetization (M) versus the applied magnetic field (H) for $MnFe_2O_4$ and $MnFe_2O_4$/PANi nanocomposite (15 wt%), respectively. The magnetic properties of the ferrite coated PS latex were analyzed by room temperature VSM with an applied

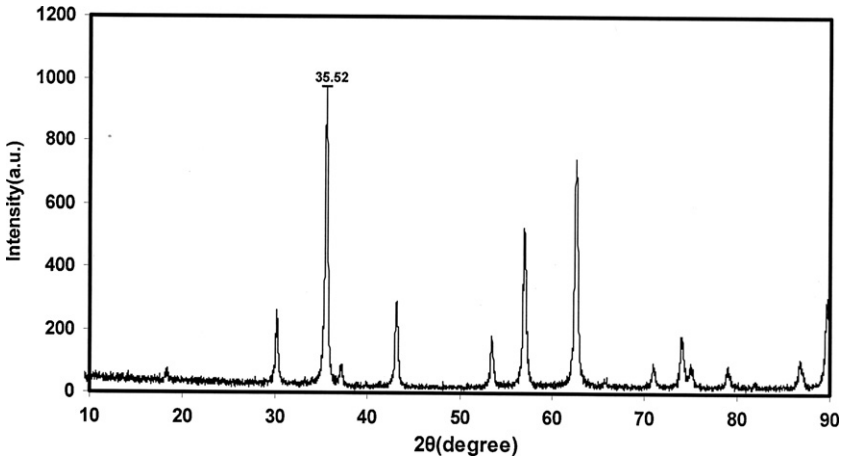

Fig. 1. X-ray diffraction for $MnFe_2O_4$.

field $-10\,kOe \leq H \leq 10\,kOe$. It can be inferred from the hysteresis loops that all the composite magnetic spheres are magnetically soft at room temperature. The value of saturation magnetization (M_s) is about 66.7 emu/g, the remnant magnetization (M_r) and coercivity field are 17.81 emu/g and 110 Oe, respectively. Fig. 2(b) shows clear saturation between $-10 \leq H \leq 10\,kOe$ with saturation magnetization (M_s) about 1.59 emu/g and the remnant magnetization (M_r) about 0.35 emu/g for nanocomposite which is lower than pure

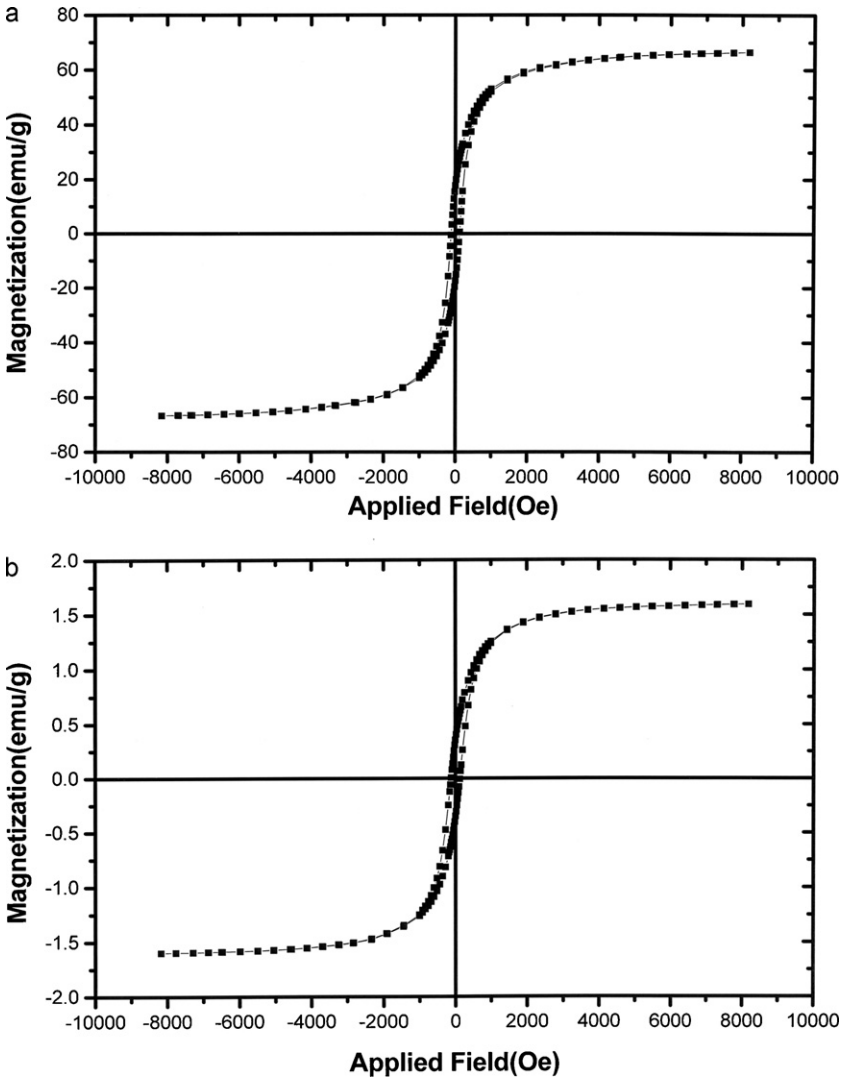

Fig. 2. Magnetic hysteresis loop of (a) $MnFe_2O_4$ nanoparticle and (b) $MnFe_2O_4$/PANi nanocomposite.

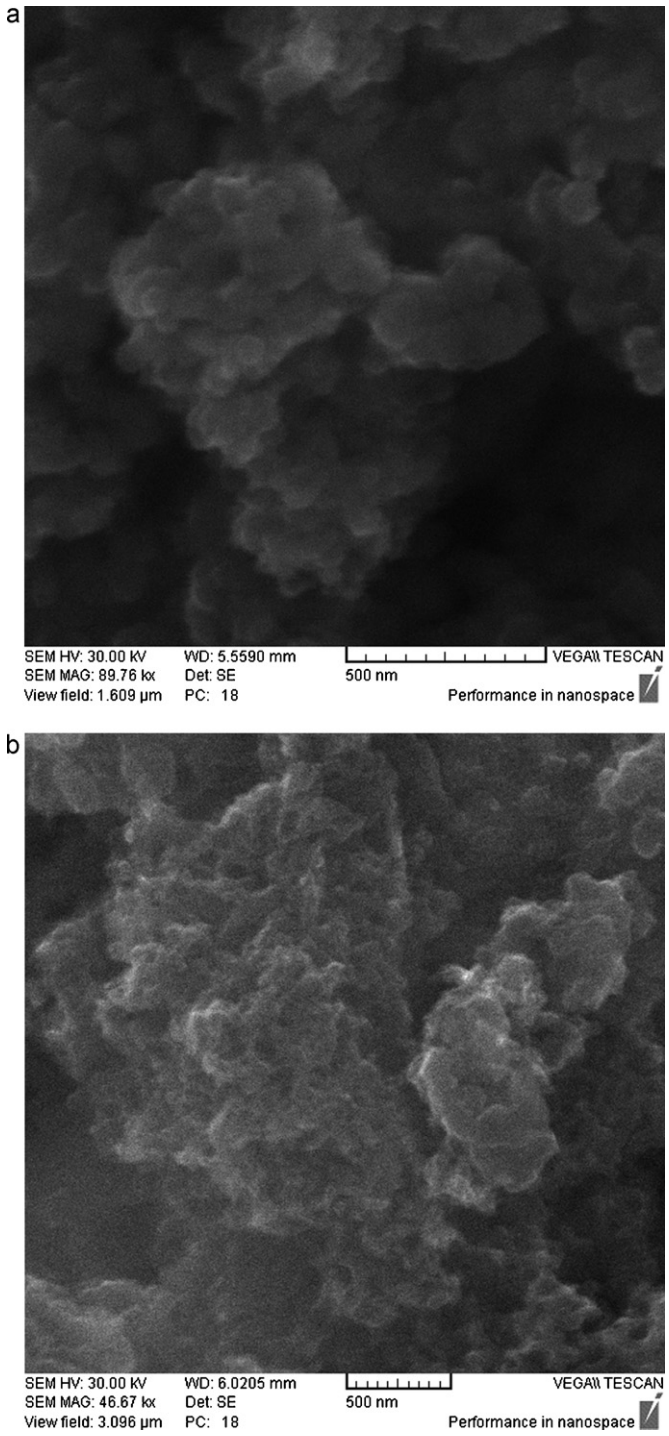

Fig. 3. SEM microphotographs of (a) $MnFe_2O_4$ nanoparticle and (b) $MnFe_2O_4$/PANi nanocomposite.

manganese ferrite nanoparticles, so the magnetization curve of the sample shows weak ferromagnetic behavior, with slender hysteresis. Magnetic properties of nanocomposites containing magnetite or ferrite particles have been believed to be highly dependent on the sample shape, crystallinity, and the value of magnetic particles, so that they can be adjusted to obtain optimum property.

3.3. Morphology investigation

Fig. 3(a) and (b) shows the SEM images for the $MnFe_2O_4$ and $MnFe_2O_4$/PANi nanocomposite, respectively. As shown in Fig. 3(a), the spongy-shaped $MnFe_2O_4$ was seen with a small quantity of amorphous phase. The length of spongy-shaped $MnFe_2O_4$ is about 80–90 nm, and the average diameter is in the range of 50–60 nm. In Fig. 3(b), it is found that the $MnFe_2O_4$/PANi nanocomposite (15 wt%) still retains the morphology of PANi shape. It is much unknown how to form spony-shaped composite in the polymerization process. The SEM image clearly shows that the $MnFe_2O_4$ was distributed rather homogeneously and ultrasonication is effective for dispersing nanoferrite in the polymer matrix.

3.4. FTIR spectra

Fig. 4(a) and (b) shows that FTIR spectra of $MnFe_2O_4$ and PANi–manganese ferrite nanocomposite, respectively. In ferrites, the metal ions are usually situated in two different sublattices, designated as tetrahedral and octahedral sites according to the geometrical configuration of the oxygen nearest neighbors [8]. It was observed from Fig. 4(a) that the peak at 570.22 cm^{-1} is intrinsic vibrations of manganese ferrite. The characteristic peaks of styrene occur at 1638, 1458.04, 1008.65–382.16, 811.30 and 865.50 cm^{-1}. The peak at 1638 is attributed to the styrene ring. The peak at 1458 cm^{-1} is attributed to the characteristic C=C stretching ring. The peaks at 811.30 and 865.50 cm^{-1} are related to the C–H outer bending vibrations.

As shown in Fig. 4(b), the characteristic peaks of PANi–manganese ferrite nanocomposite occur at 1559.20, 1479.72, 1302.68, 1241.25, 1125.64, 1031.70, 1006.41–796.85, 576.45 cm^{-1}. The peaks at 1559.20 and 1479.72 cm^{-1} are attributed to the characteristic C=C and C–N stretching of the quinoid and benzenoid rings of polyaniline; the peaks at 1302.68 and 1241.25 cm^{-1} correspond to N–H bending and asymmetric C–N stretching modes of the benzenoid ring, respectively. The peak around 1125.64 cm^{-1} is associated with vibrational modes of N=Q=N (Q refers to the quinonic type rings), indicating that PANi is formed in our sample. The peak at 1031.70 cm^{-1} attributed to the symmetric and anti-symmetric stretching vibration of SO_3 group of dopant (DBSA). The peaks at 1006.41–796.85 cm^{-1} are attributed to the p-disubstituted aromatic ring C–H out-of-plane bending. However, the characteristic peaks of $MnFe_2O_4$ can be observed at higher wave numbers (576.45 cm^{-1}) indicating that there is an interaction between $MnFe_2O_4$ particles and PANi chains.

3.5. TEM analysis

Average particle size of the manganese ferrite powders measured using TEM analysis and micrographs for the powder are shown in Fig. 5. The photographs indicate that average particle size of the powders was in the 20–30 nm range. Particles were uniformly elongated and formed loose aggregates.

3.6. Microwave absorbing properties

Nanocomposite powders dispersed in acrylic resins then the mixture was pasted on metal plate with the area of 100 mm × 100 mm as the test plate. The microwave absorbing properties of the nanocomposite with the coating thickness of 1.4 mm were investigated by using vector network analyzers in the frequency range of 8–12 GHz. Fig. 6 shows the variation of reflection loss versus frequency determined from PANi–manganese ferrite nanocomposite. For $MnFe_2O_4$ composites with the coating thickness of 1.5 mm the reflection loss values less than −10 dB were obtained in the frequency of 8–12 GHz and its value of minimum reflection loss is −15.3 dB at the frequency of 10.4 GHz.

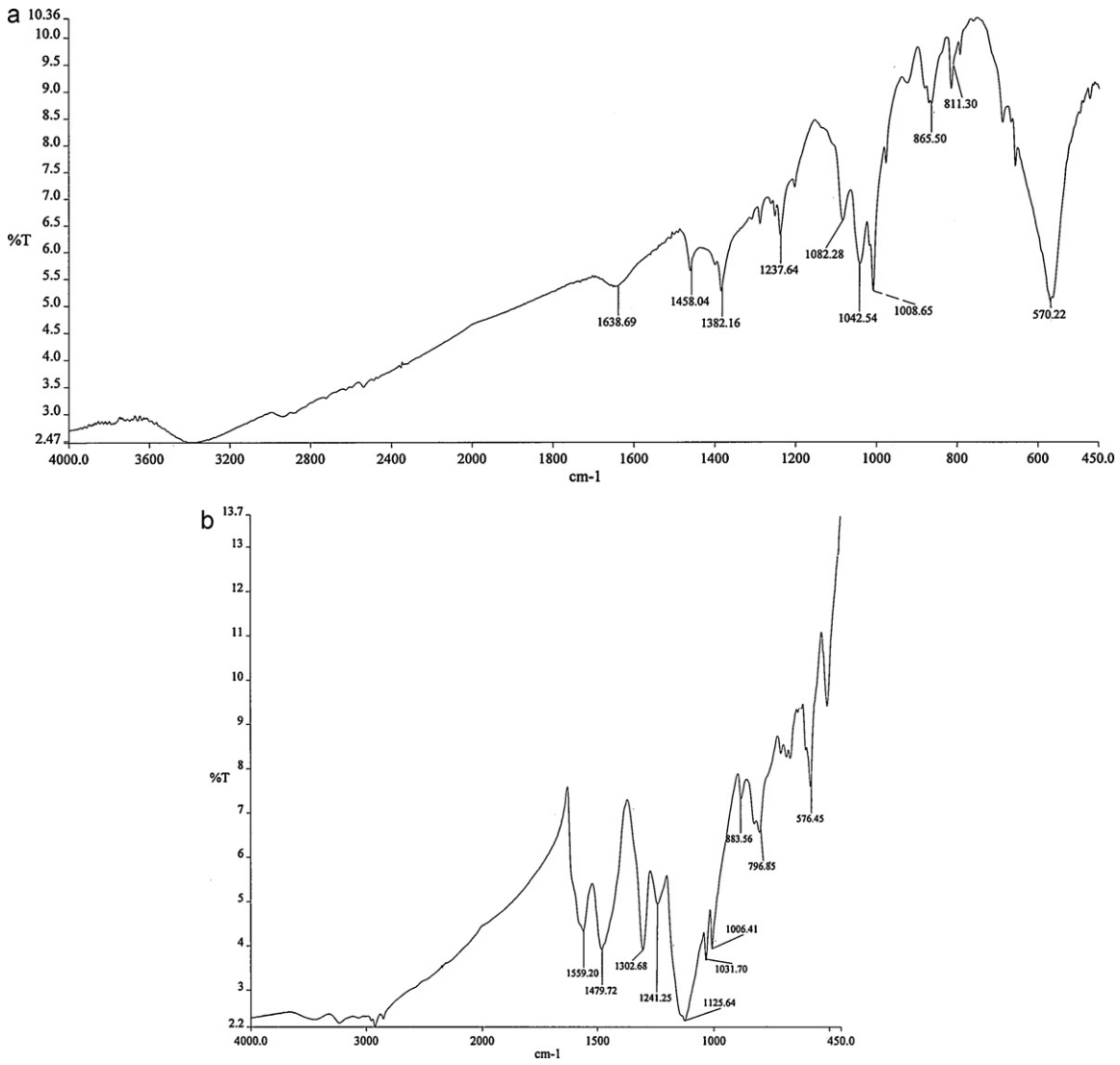

Fig. 4. FTIR spectra: (a) $MnFe_2O_4$ nanoparticle and (b) $MnFe_2O_4$/PANi nanocomposite.

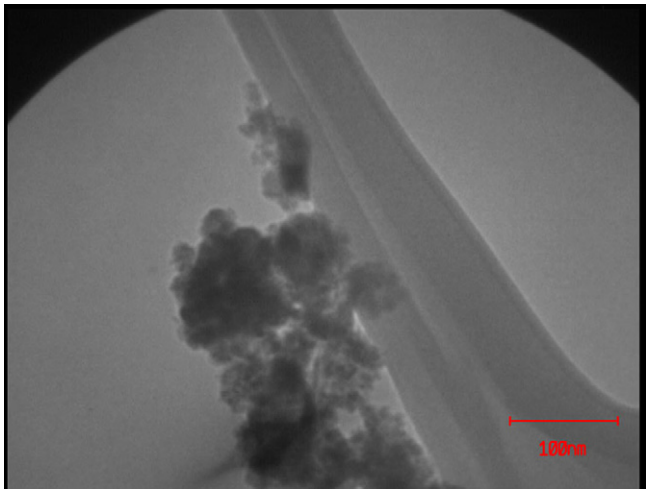

Fig. 5. TEM images of $MnFe_2O_4$ nanoparticle.

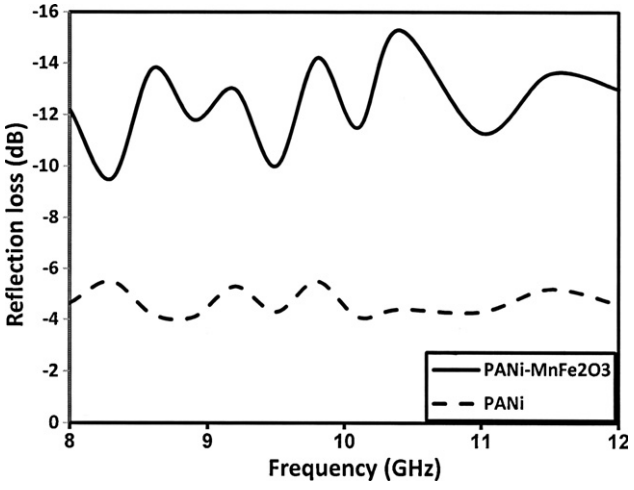

Fig. 6. Frequency dependence of RL for the $MnFe_2O_4$/PANi nanocomposite.

4. Conclusions

The obtained magnetic nanoparticles are of a diameter of 24.27 nm. PANi–manganese ferrite nanocomposite with the magnetic behavior is successfully synthesized by in situ polymerization of aniline in the presence of $MnFe_2O_4$ nanoparticles. The results of spectro-analysis indicate that there is an interaction between PANi chains and ferrite particles. A minimum reflection loss of −15.3 dB was observed at 10.4 GHz with at thickness of 1.4 mm of nanocomposite.

References

[1] Z. Wang, H. Bi, J. Liu, T. Sun, X. Wu, J. Magn. Magn. Mater. 320 (2008) 2132.
[2] L. Jing, G. Wang, Y. Duan, Y. Jiang, J. Alloys Compd. 475 (2009) 862.
[3] A.C.F.M. Costa, A.P. Diniz, V.J. Silva, R.H.G.A. Kiminami, D.R. Cornejo, A.M. Gamad, M.C. Rezended, L. Gama, J. Alloys Compd. 483 (2009) 563.
[4] S.W. Phang, M. Tadokoro, J. Watanabe, N. Kuramoto, Curr. Appl. Phys. 8 (2008) 391.
[5] K. Singh, A. Ohlan, A.K. Bakhshi, S.K. Dhawan, Mater. Chem. Phys. 119 (2010) 201.
[6] Y. Li, H. Zhang, Y. Liu, Q. Wen, J. Li, Nanotechnology 19 (2008) 105605.
[7] K. Lakshmi, H. John, K.T. Mathew, R. Joseph, K.E. George, Acta Mater. 57 (2009) 371.
[8] S.P. Gairola, V. Verma, L. Kumar, M.A. Dar, S. Annapoorni, R.K. Kotnala, Synth. Met. 160 (2010) 2315.
[9] T.H. Ting, K.H. Wu, J. Magn. Magn. Mater. 322 (2010) 2160.
[10] H.M. Xiao, W.D. Zhang, S.Y. Fu, Compos. Sci. Technol. 70 (6) (2010) 909.
[11] H. MeiXiao, X.M. Liu, S.Y. Fu, Compos. Sci. Technol. 66 (2006) 2003.
[12] S.M. Abbas, A.K. Dixit, R. Chatterjee, T.C. Goel, Mater. Sci. Eng. B 123 (2005) 167.
[13] D.A. Makeiff, T. Huber, Synth. Met. 156 (2006) 497.
[14] D.L. Zhao, F. Luo, W.C. Zhou, J. Alloys Compd. 490 (2010) 190.
[15] Y.L. Cheng, J.M. Dai, D.J. Wu, Y.P. Sun, J. Magn. Magn. Mater. 322 (2010) 97.
[16] Z.B. Huang, F.Q. Tang, Colloid Polym. Sci. 282 (2004) 1198.